



HAL
open science

On the combustion of terpenes biofuels

Philippe Dagaut, Zahraa Dbouk, Nesrine Belhadj, Maxence Lailliau, Roland Benoit

► **To cite this version:**

Philippe Dagaut, Zahraa Dbouk, Nesrine Belhadj, Maxence Lailliau, Roland Benoit. On the combustion of terpenes biofuels. INFUB-14, CENERTEC, Apr 2024, Algrave, Portugal. hal-04528441v2

HAL Id: hal-04528441

<https://hal.science/hal-04528441v2>

Submitted on 30 Apr 2024

HAL is a multi-disciplinary open access archive for the deposit and dissemination of scientific research documents, whether they are published or not. The documents may come from teaching and research institutions in France or abroad, or from public or private research centers.

L'archive ouverte pluridisciplinaire **HAL**, est destinée au dépôt et à la diffusion de documents scientifiques de niveau recherche, publiés ou non, émanant des établissements d'enseignement et de recherche français ou étrangers, des laboratoires publics ou privés.

Public Domain

On the combustion of terpenes biofuels

Philippe Dagaut*, Zahraa Dbouk*, Nesrine Belhadj*, Maxence Laillau* and Roland Benoit*

philippe.dagaut@cnrso-orleans.fr

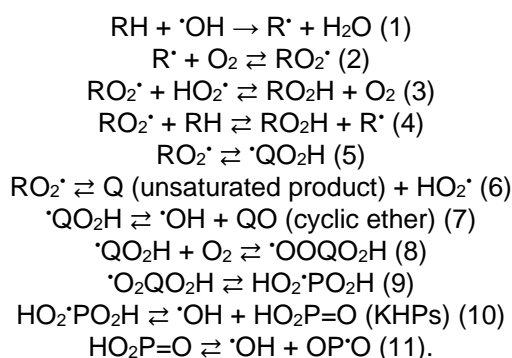
*CNRS-INSIS, ICARE, Orléans, France

Abstract

Limonene, α -pinene, and β -pinene, which can be used as biofuel components for engines and boilers, were oxidized in a jet-stirred reactor at atmospheric pressure, in the cool flame regime, and under fuel-lean conditions. Samples of the reacting mixtures were drawn from the reactor, dissolved in acetonitrile, and analyzed by high-resolution mass spectrometry. In order to characterize the oxidation products, direct flow injection or chromatographic separation by ultra-high-performance liquid chromatography and +/- heated electrospray ionization and +/- atmospheric pressure chemical ionization were completed. H/D exchange using D₂O was used for assessing the presence of hydroxyl and hydroperoxyl functional groups in the oxidation products. The presence of carbonyl functional groups in the products was verified by reacting the samples with 2,4-dinitrophenylhydrazine. A large set of oxidation products, including highly oxygenated organics, was observed. Van Krevelen plots, oxidation state of carbon, degree of unsaturation and aromaticity index were used to rationalize the results and helped to demonstrate the production of aromatic and/or polyunsaturated chemicals.

Introduction

The terpenes are a class of hydrocarbons naturally released by vegetation. They represent a large portion of volatile organic chemicals (VOCs) present in the troposphere [1, 2]. In addition, because of their high-energy-density, they could be used as a biofuel [3, 4]. The monoterpenes with cetane numbers around 20 could be used as drop-in fuel to lessen transportation carbon footprint as well as that of boilers. Nevertheless, using terpenes as biofuel or drop-in fuel could increase their concentration in air through fuel evaporation and unburnt fuel emissions. Whereas the kinetics of oxidation of several terpenes under conditions relevant to the troposphere has been extensively studied [5, 6], the understanding of the numerous and intricate oxidation routes has not been reached yet [5-7]. The chemical kinetics of combustion of this class of hydrocarbons has received little attention up to now. Indeed, only burning velocities in air, flame structures, and impact on ignition have been published [8-10]. It has been recognized that the combustion of hydrocarbons (RH) produces a range of oxygenated products such as ketohydroperoxides (KHPs) which are responsible for chain branching under cool-flame conditions through a sequence of chemical reactions [11] (see Figure 1):



In the recent years, the formation of more oxygenated products in cool flames was observed for a wide range of fuels [12, 13]. These products are formed via alternative oxidation routes which involve an internal H-transfer in $\cdot\text{O}_2\text{QO}_2\text{H}$ radicals. This H-transfer occurs on another H-C group rather than on the H-COOH group which is responsible for KHPs formation (Reactions 9 and 10). Then, it opens new oxidation pathways including at least a third O₂ addition to HO₂·PO₂H yielding $\cdot\text{O}_2\text{P}(\text{O}_2\text{H})_2$. This sequence of reactions, i.e., H-transfer and O₂ addition can occur several times, yielding highly oxidized

products [12]. Also, $\cdot\text{QO}_2\text{H}$ radicals will decompose yielding stable products and radicals via Reaction (7) and:

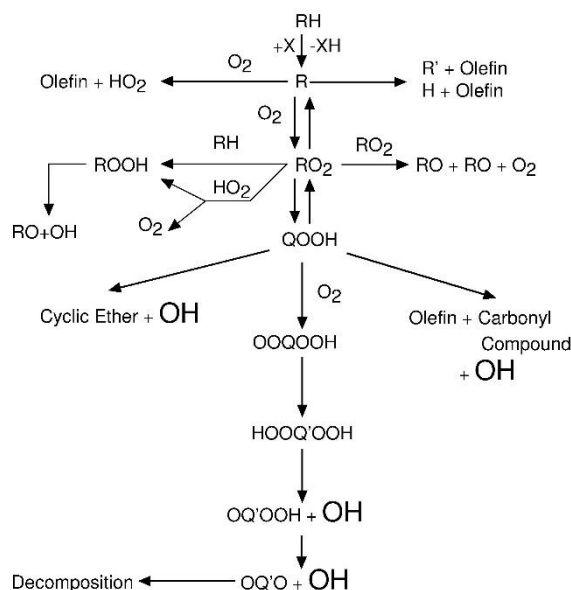
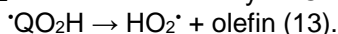
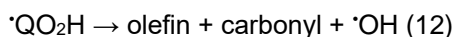
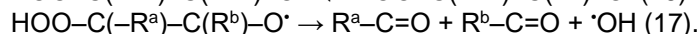
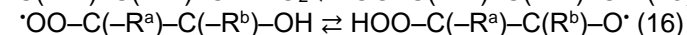
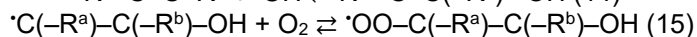


Figure 1. Simplified hydrocarbons oxidation scheme.

In the case of unsaturated hydrocarbons such as terpenes, oxidation via the Waddington mechanism [14] can occur. The reaction starts by $\cdot\text{OH}$ addition on a $\text{C}=\text{C}$ double bond followed by O_2 addition and internal H-atom transfer from the $-\text{OH}$ group to the $-\text{OO}\cdot$ peroxy group, followed by decomposition:



In this reaction mechanism, the hydroxyl radical initially consumed in Reaction (14) is regenerated in Reaction (17).

The Korcek mechanism [14] which transforms γ -keto hydroperoxides into a carbonyl and a carboxylic acid, can also contribute to the oxidation of the fuel, as shown in recent combustion kinetic modeling [15, 16]. Finally, other reaction pathways, such as the production of aromatics during the cool flame oxidation of monoterpenes, have not received much attention.

This work aims to better characterize the autoxidation products of terpenes (limonene, α -pinene, and β -pinene, see Fig. 2) under cool-flame conditions and examine the formation of aromatics. To achieve these goals, we performed oxidation experiments in a jet-stirred reactor at 1 bar, and oxidation products were characterized using high-resolution mass spectrometry.

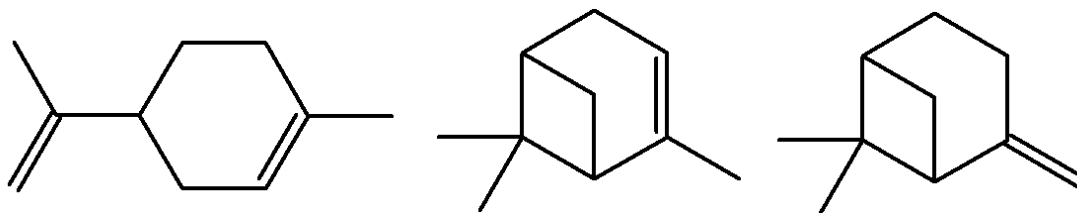


Figure 2. Chemical structure of limonene, α -pinene, and β -pinene (from left to right)

Experimental

Experiments were conducted in a 42 mL fused silica jet-stirred-reactor (JSR) presented in previous papers [17, 18]. As before [19, 20] for injecting the fuels in the JSR, we used a HPLC pump with an online degasser. The fuels were delivered to an in-house vaporizer assembly fed with a flow of N_2 . Fuel- N_2 and O_2 - N_2 flowed separately to the JSR to avoid premature oxidation. Mass flow meters were used to deliver the flow rates of N_2 and O_2 . A thermocouple (0.1 mm Pt-Pt/Rh-10% wires protected by a thin silica tube) was moved along the vertical axis of the JSR to verify thermal homogeneity (gradients of < 1 K/cm). We performed experiments in the cool-flame regime (520-680 K). One percent of fuel was oxidized at 1 bar, in fuel-lean conditions ($\phi = 0.25$), and at a mean residence time of 2 s.

The products of oxidation were dissolved through bubbling into 250 mL of acetonitrile (≥ 99.9 pure, 273 K) for 90 min (Fig. 3). They were stored in a freezer at 258 K for further chemical analyses. Flow injection analyses with heated electrospray ionization (FIA/HESI) were performed. The samples were analyzed by Orbitrap Q-Exactive (high-resolution mass spectrometry, HRMS). Mass calibrations in positive and negative modes were done by injecting \pm HESI calibration mixtures. Reverse-phase ultra-high-performance liquid chromatography (RP-UHPLC) analyses were conducted using a C18 analytical column (Phenomenex Luna, 1.6 μ m, 100 \AA , 100x2.1 mm). 3 μ L of samples were eluted by water-acetonitrile (ACN) mix at a flow rate of 250 μ L/min (gradient 5% to 90% ACN, during 33 min). Also, atmospheric pressure chemical ionization (APCI) was used in positive and negative modes. For determining the chemical structure of oxidation products after RP-UHPLC separation, MS/MS analyses were performed using the lowest collision cell energy (10 eV). As previously [19, 20] 2,4-dinitrophenylhydrazine (2,4-DNPH) addition to samples was also used to assess the presence of carbonyl compounds. As in previous studies [12, 19-21], we evaluated the presence of hydroxyl ($-\text{OH}$) or hydroperoxyl ($-\text{OOH}$) groups in the products by performing H/D exchange by addition of D_2O into the samples. These solutions were analyzed by FIA-HESI-HRMS and RP-UHPLC-APCI-HRMS.

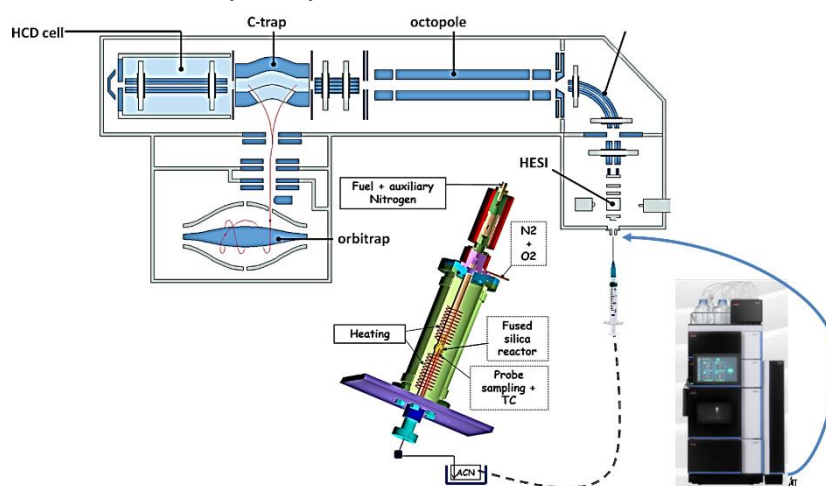


Figure 3. Schematic presentation of the experimental setup used.

Results and Discussion

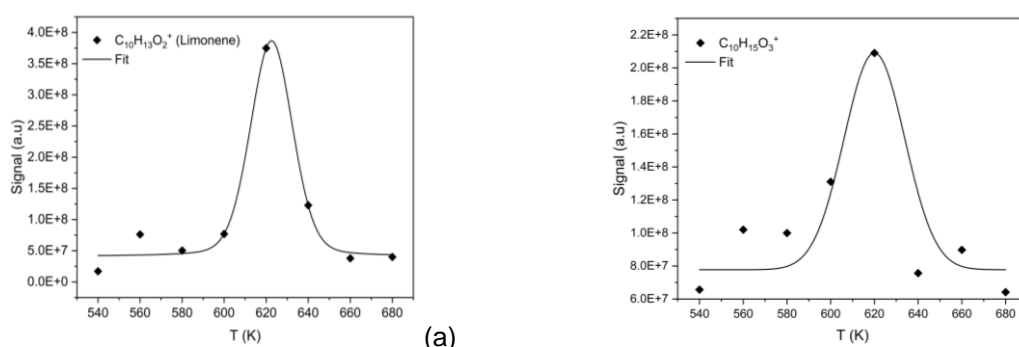


Figure 4. Products of oxidation of (a) limonene and (b) β -pinene obtained by HRMS (symbols). The data for KHPs and isomers ($C_{10}H_{14}O_3$) were obtained by FIA and HESI (+), i.e., $C_{10}H_{15}O_3^+$, m/z 183.1015.

Many oxidation products were detected during the oxidation of the three terpenes. Oxidation products, containing ≥ 1 O-atom, were detected: $C_7H_{10}O_{4,5}$, $C_8H_{12}O_{2,4}$, $C_8H_{14}O_{2,4}$, $C_9H_{12}O$, $C_9H_{14}O_{1,3-5}$, $C_{10}H_{12}O_2$, $C_{10}H_{14}O_{1-9}$, $C_{10}H_{16}O_{2-5}$, and $C_{10}H_{18}O_6$. Figure 4 shows results obtained for KHPs and their isomers. As can be seen from that figure, the products peak at a temperature ~ 620 K. H/D exchange and reaction with 2,4-DNPH were used to assess the presence of OOH and C=O functional groups in the $C_{10}H_{14}O_3$ products. Carbonyl compounds formed through the Waddington mechanism on C=C double bonds of the fuels were observed as well as their oxidation products.

As mentioned in the Introduction, products of the Korcek mechanism are carboxylic acids and carbonyls. Such products were also detected in this work. Among the 18 KHPs deriving from limonene oxidation, four isomers could decompose via the Korcek mechanism. However, only one isomer can possibly yield a cyclic intermediate peroxide linking the carbonyl and OOH groups which yields a carbonyl compound, $C_9H_{12}O$, and formic acid, CH_2O_2 , by decomposition (Fig. 5). Both products were detected by UHPLC-HRMS in this study. For the two other terpenes, we also observed products of the Korcek mechanism.

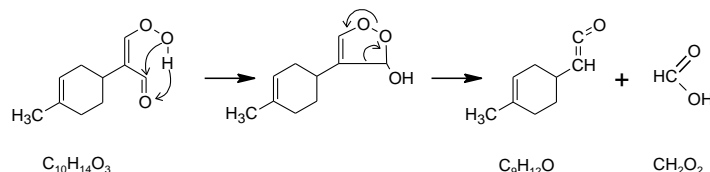


Figure 5. Example of the Korcek mechanism during limonene oxidation.

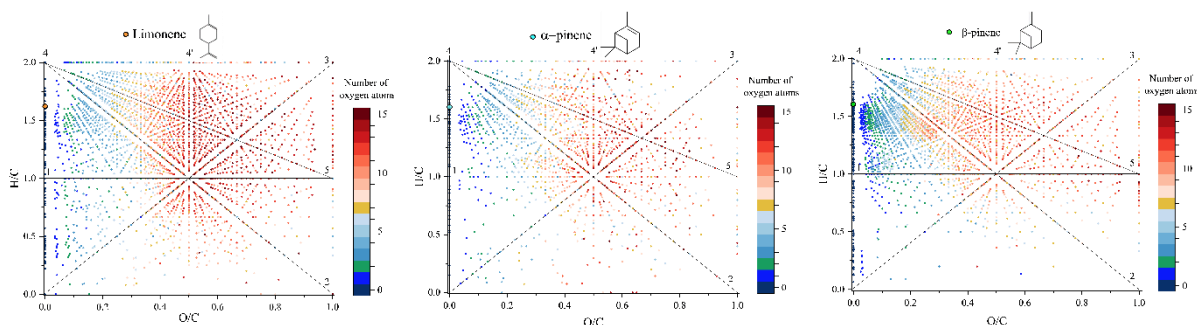


Figure 6. Van Krevelen plot for limonene, α -pinene, and β -pinene oxidation products (sampled at 590 K). Lines indicate 1: oxidation, 2: carbonylation, 3: hydration, 4: dehydrogenation, 5: carboxylation, or reverse processes [22]. Color-coding indicates the number of O-atoms in chemical formulas.

The formation of C_nH_2 , C_nH_4 , and C_nH_6 ($n \geq 4$) isomers was observed for the terpene fuels on line 4 with $O/C = 0$ in Van Krevelen (VK) plots using HESI+/- FIA-HRMS data (Fig. 6; the position of the fuels is shown as a circle). These plots indicated the formation of aromatics ($H/C < 0.7$ and $O/C = 0$) and polyunsaturated products. In the space defined by $0 < O/C < 0.2$ and $H/C \leq 1$, we observed products of oxidation (line 1) and dehydrogenation (line 4). For $H/C < 1$, the degree of oxidation of products is less than for $H/C > 1$.

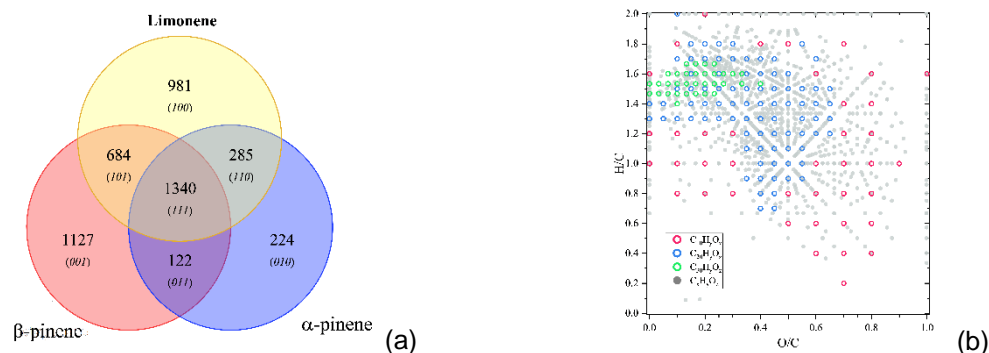


Figure 7. (a) Venn diagram showing common chemical formulas observed for each fuel. (b) VK plot of chemical formulas common to the three fuels.

In Figure 7, we plotted the data obtained for the three fuels in a Venn diagram. One can see from that figure that 1340 common chemical formulas are found in the products of oxidation of the three fuels. Common chemical formulas are also observed for two fuels, whereas a large fraction of chemical formulas is found specifically for limonene and β -pinene. In order to further analyse the results, we used a VK plot limited to chemical formulas detected in the products of the three fuels. One can see from that figure that these chemical formulas are present in all the regions of the VK diagram. Nevertheless, one could note that C30 chemicals are located in the space $0 < O/C < 0.4$ and $H/C > 1.4$.

In order to further characterize the oxidation products, the percentage of unsaturation was computed using the following equation: $(3 \times C + 1) / (C - H/2 + 1)$, where H and C represent the number of hydrogen and C-atoms, respectively. Plotting the percentage of unsaturation versus the number of carbon atoms in the detected products (Fig. 8) confirms that high degrees of unsaturation are reached and the products mass range extends over m/z 550.

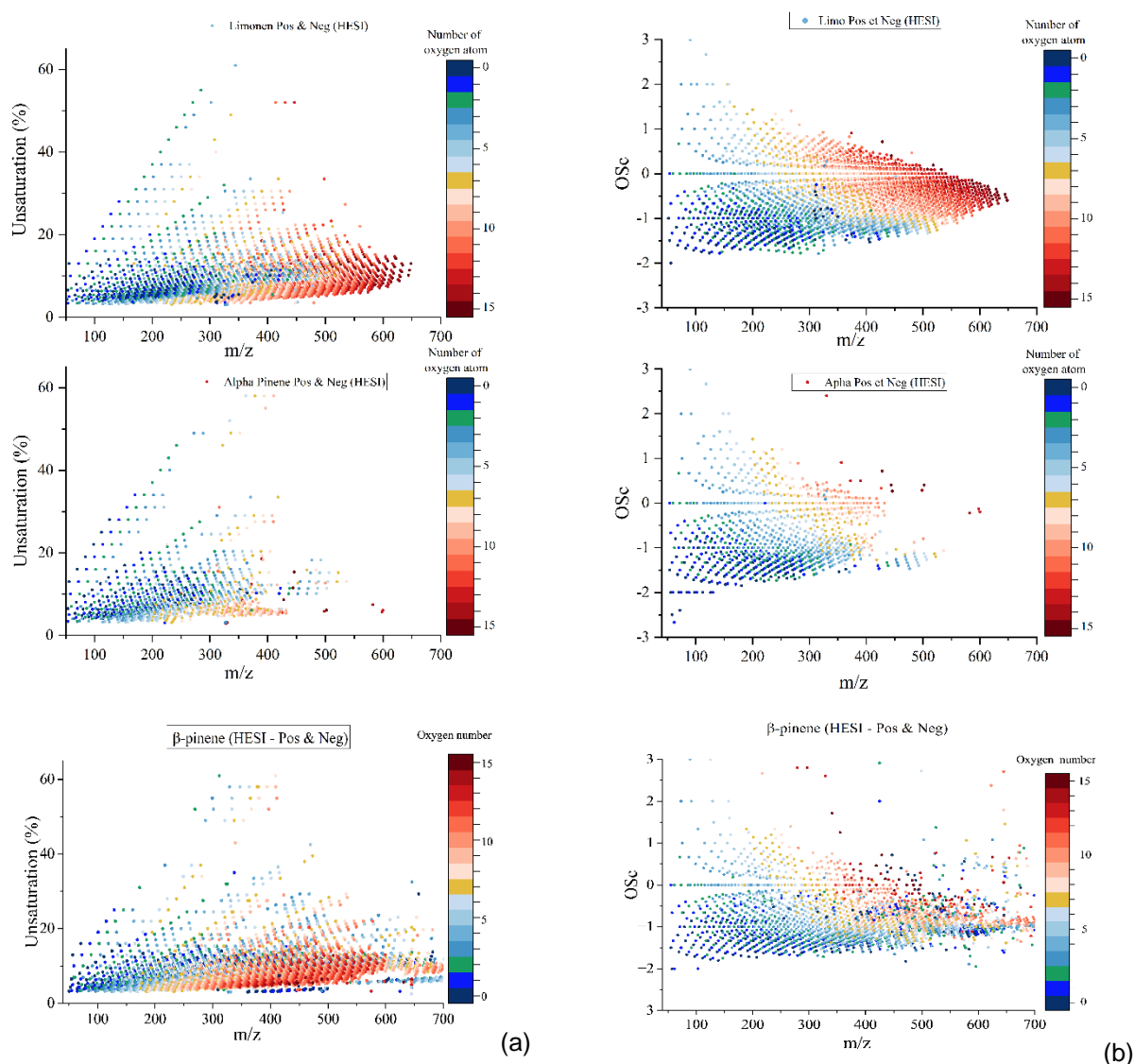


Figure 8. (a) Variation of the degree of unsaturation in the oxidation products of limonene (top), α -pinene (middle), and β -pinene (bottom). (b) Overview of the distribution of limonene (top), α -pinene (middle), and β -pinene (bottom) oxidation products observed (+/- HESI) by plotting OSc versus carbon number in detected chemical formulae. $OSc \approx 2 O/C - H/C$ [23] where H , C , and O represent the number of hydrogen, carbon, and oxygen atoms, respectively. Color-coding indicates the number of O-atoms in chemical formulas.

Below m/z 550, similar trends are observed for all fuels, although the data show significantly more products with high m/z in the case of limonene, which could be due to the presence of both *endo* and *exo* C=C bonds in limonene. These data were obtained under the following conditions: HESI+/-, FIA-HRMS (sample taken at 580 K). Whereas the presently observed formation of aromatics and polyunsaturated products under cool-flame conditions was rather unexpected, it should be investigated further under simulated atmospheric oxidation conditions since the oxidation of aromatics could significantly contribute to the formation of secondary organic aerosols.

The oxidation state of carbon (OSc) in products was also studied (Fig. 8). Besides the fact that higher m/z oxidation products were detected in limonene and β -pinene oxidation samples, similar trends were observed for all fuels. For OSc < -1 and m/z > 200, aromatic products are likely present.

To better assess the presence of different chemical classes in oxidation products of limonene, α -pinene, and β -pinene, we computed the aromaticity index (AI) and defined chemical families based on previous attempts in the literature [24]: aliphatic compounds ($A \leq 0$), olefinic products and naphthenic compounds ($0 < AI < 0.3$) including the fuel which have an AI of 0.3, highly unsaturated compounds ($0.3 < AI \leq 0.5$), aromatics ($0.5 < AI \leq 0.67$), and polyaromatics ($0.67 < AI$). As can be seen from Figure 9, for limonene, α -pinene, and β -pinene a significant fraction of aromatics and polyaromatics is present in the oxidation products.

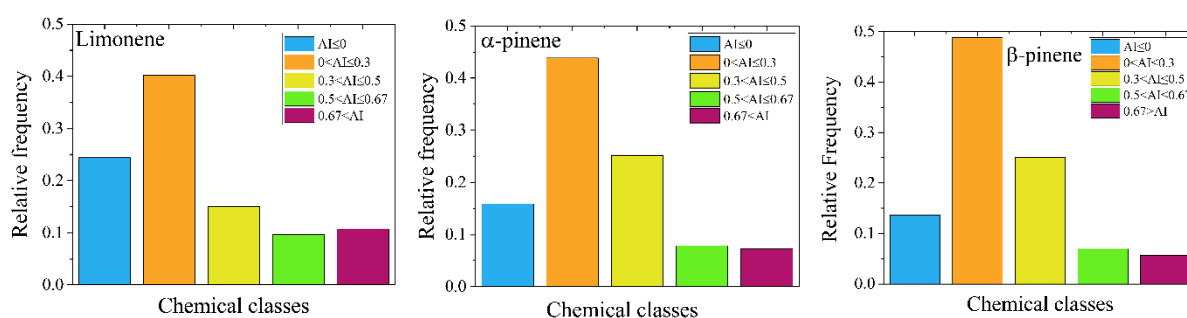


Figure 9. Chemical classes found in the oxidation products of limonene, α -pinene, and β -pinene.

$AI_{mod} = (1 + C - 0.5 \times O - 0.5 \times H) / (C - 0.5 \times O)$, where C , H , and O represent the number of carbon, hydrogen, and oxygen atoms, respectively, in the chemical formulas [25, 26].

Summary

Fuel-lean mixtures of limonene, α -pinene, and β -pinene were oxidized in a JSR at 1 bar, in the cool flame regime. The reacting mixtures were sampled. Gases were dissolved in acetonitrile through bubbling and analyzed by high-resolution mass spectrometry after soft ionization. Direct flow injection or chromatographic separation using UHPLC and +/- HESI and +/- APCI allowed characterizing the oxidation products. H/D exchange and reaction with 2,4-DNPH were used to assess the presence of OOH (or OH) and C=O functions in the oxidation products. A large set of chemical formulas was observed. Among them, highly oxygenated products were detected. Van Krevelen plots, oxidation state of carbon, aromaticity index, and degree of unsaturation were used to characterize the oxygenated products and demonstrate the formation of aromatic and/or polyunsaturated products during the cool flame oxidation of terpenes.

References

- [1] Seinfeld, JH, Pandis, SN, *Atmospheric Chemistry and Physics: From Air Pollution to Climate Change*, 2nd ed.; Wiley-Interscience: Hoboken, NJ, 2006.
- [2] Zhang, H, Yee, LD, Lee, BH, Curtis, MP, Worton, DR, Isaacman-VanWertz, G, Offenberg, JH, Lewandowski, M, Kleindienst, TE, Beaver, MR, Holder, AL, Lonneman, WA, Docherty, KS, Jaoui, M, Pye, HOT, Hu, W, Day, DA, Campuzano-Jost, P, Jimenez, JL, Guo, H, Weber, RJ, de Gouw, J, Koss, AR, Edgerton, ES, Brune, W, Mohr, C, Lopez-Hilfiker, FD, Lutz, A, Kreisberg, NM, Spielman, SR, Hering, SV, Wilson, KR, Thornton, JA, Goldstein, AH, "Monoterpenes are the largest source of summertime organic aerosol in the southeastern United States", *Proceedings of the National Academy of Sciences*, 115, 2018, 2038-2043.
- [3] Pourbafrani, M, Forgács, G, Horváth, IS, Niklasson, C, Taherzadeh, MJ, "Production of biofuels, limonene and pectin from citrus wastes", *Bioresour. Technol.*, 101, 2010, 4246-4250.

- [4] Mewalal, R, Rai, DK, Kainer, D, Chen, F, Külheim, C, Peter, GF, Tuskan, GA, "Plant-Derived Terpenes: A Feedstock for Specialty Biofuels", *Trends Biotechnol.*, **35**, 2017, 227-240.
- [5] Benoit, R, Belhadj, N, Dbouk, Z, Lailliau, M, Dagaut, P, "On the formation of highly oxidized pollutants by autoxidation of terpenes under low-temperature-combustion conditions: the case of limonene and α -pinene", *Atmos. Chem. Phys.*, **23**, 2023, 5715-5733.
- [6] Benoit, R, Belhadj, N, Lailliau, M, Dagaut, P, "Autoxidation of terpenes, a common pathway in tropospheric and low temperature combustion conditions: the case of limonene and α -pinene", *Atmos. Chem. Phys. Discuss.*, 2021, 2021, 1-21.
- [7] Berndt, T, Richters, S, Kaethner, R, Voigtländer, J, Stratmann, F, Sipilä, M, Kulmala, M, Herrmann, H, "Gas-phase ozonolysis of cycloalkenes: formation of highly oxidized RO₂ radicals and their reactions with NO, NO₂, SO₂, and other RO₂ radicals", *The Journal of Physical Chemistry A*, **119**, 2015, 10336-10348.
- [8] Chetehouna, K, Courty, L, Mounaim-Rousselle, C, Halter, F, Garo, J-P, "Combustion Characteristics of p-Cymene Possibly Involved in Accelerating Forest Fires", *Combust. Sci. Technol.*, **185**, 2013, 1295-1305.
- [9] Courty, L, Chetehouna, K, Halter, F, Foucher, F, Garo, JP, Mounaim-Rousselle, C, "Experimental determination of emission and laminar burning speeds of alpha-pinene", *Combust. Flame*, **159**, 2012, 1385-1392.
- [10] Bierkandt, T, Hoener, M, Gaiser, N, Hansen, N, Koehler, M, Kasper, T, "Experimental flat flame study of monoterpenes: Insights into the combustion kinetics of alpha-pinene, beta-pinene, and myrcene", *Proc. Combust. Inst.*, **38**, 2021, 2431-2440.
- [11] Morley, C, "A Fundamentally Based Correlation Between Alkane Structure and Octane Number", *Combust. Sci. Technol.*, **55**, 1987, 115-123.
- [12] Wang, Z, Popolan-Vaida, DM, Chen, B, Moshhammer, K, Mohamed, SY, Wang, H, Sioud, S, Raji, MA, Kohse-Höinghaus, K, Hansen, N, Dagaut, P, Leone, SR, Sarathy, SM, "Unraveling the structure and chemical mechanisms of highly oxygenated intermediates in oxidation of organic compounds", *Proceedings of the National Academy of Sciences*, **114**, 2017, 13102-13107.
- [13] Wang, ZD, Chen, BJ, Moshhammer, K, Popolan-Vaida, DM, Sioud, S, Shankar, VSB, Vuilleumier, D, Tao, T, Ruwe, L, Brauer, E, Hansen, N, Dagaut, P, Kohse-Hoinghaus, K, Raji, MA, Sarathy, SM, "n-Heptane cool flame chemistry: Unraveling intermediate species measured in a stirred reactor and motored engine", *Combust. Flame*, **187**, 2018, 199-216.
- [14] Ray, DJM, Redfean, A, Waddington, DJ, "Gas-phase oxidation of alkenes: decomposition of hydroxy-substituted peroxy radicals", *Journal of the Chemical Society, Perkin Transactions 2*, 1973, 540-543.
- [15] Ranzi, E, Cavallotti, C, Cuoci, A, Frassoldati, A, Pelucchi, M, Faravelli, T, "New reaction classes in the kinetic modeling of low temperature oxidation of n-alkanes", *Combust. Flame*, **162**, 2015, 1679-1691.
- [16] Xie, C, Lailliau, M, Issayev, G, Xu, Q, Chen, W, Dagaut, P, Farooq, A, Sarathy, SM, Wei, L, Wang, Z, "Revisiting low temperature oxidation chemistry of n-heptane", *Combust. Flame*, **242**, 2022, 112177.
- [17] Dagaut, P, Cathonnet, M, Rouan, JP, Foulatier, R, Quilgars, A, Boettner, JC, Gaillard, F, James, H, "A jet-stirred reactor for kinetic studies of homogeneous gas-phase reactions at pressures up to ten atmospheres (≈ 1 MPa)", *Journal of Physics E: Scientific Instruments*, **19**, 1986, 207-209.
- [18] Dagaut, P, Cathonnet, M, Boettner, JC, "Experimental-Study and Kinetic Modeling of Propene Oxidation in a Jet Stirred Flow Reactor", *J. Phys. Chem.*, **92**, 1988, 661-671.
- [19] Belhadj, N, Benoit, R, Dagaut, P, Lailliau, M, Serinyel, Z, Dayma, G, "Oxidation of di-n-propyl ether: Characterization of low-temperature products", *Proc. Combust. Inst.*, **38**, 2021, 337-344.
- [20] Belhadj, N, Lailliau, M, Benoit, R, Dagaut, P, "Towards a Comprehensive Characterization of the Low-Temperature Autoxidation of Di-n-Butyl Ether", *Molecules*, **26**, 2021, 7174.
- [21] Belhadj, N, Benoit, R, Dagaut, P, Lailliau, M, "Experimental characterization of n-heptane low-temperature oxidation products including keto-hydroperoxides and highly oxygenated organic molecules (HOMs)", *Combust. Flame*, **224**, 2021, 83-93.
- [22] Kim, S, Kramer, RW, Hatcher, PG, "Graphical Method for Analysis of Ultrahigh-Resolution Broadband Mass Spectra of Natural Organic Matter, the Van Krevelen Diagram", *Anal. Chem.*, **75**, 2003, 5336-5344.
- [23] Kroll, JH, Donahue, NM, Jimenez, JL, Kessler, SH, Canagaratna, MR, Wilson, KR, Altieri, KE, Mazzoleni, LR, Wozniak, AS, Bluhm, H, Mysak, ER, Smith, JD, Kolb, CE, Worsnop, DR,

- "Carbon oxidation state as a metric for describing the chemistry of atmospheric organic aerosol", *Nature Chemistry*, 3, 2011, 133-139.
- [24] Schneider, E, Czech, H, Popovicheva, O, Lütcke, H, Schnelle-Kreis, J, Khodzher, T, Rüger, CP, Zimmermann, R, "Molecular Characterization of Water-Soluble Aerosol Particle Extracts by Ultrahigh-Resolution Mass Spectrometry: Observation of Industrial Emissions and an Atmospherically Aged Wildfire Plume at Lake Baikal", *ACS Earth and Space Chemistry*, 6, 2022, 1095-1107.
- [25] Brege, MA, China, S, Schum, S, Zelenyuk, A, Mazzoleni, LR, "Extreme Molecular Complexity Resulting in a Continuum of Carbonaceous Species in Biomass Burning Tar Balls from Wildfire Smoke", *ACS Earth and Space Chemistry*, 5, 2021, 2729-2739.
- [26] Koch, BP, Dittmar, T, "From mass to structure: an aromaticity index for high-resolution mass data of natural organic matter", *Rapid Commun. Mass Spectrom.*, 30, 2016, 250-250.